Available online at www.sciencedirect.com
SCIENCE DIRECT®
Journal of Power Sources 140 (2005) 268–273
JOURNAL OF POWER SOURCES
www.elsevier.com/locate/jpowsour

Short communication

Effects of preparation conditions on performance of carbon-supported nanosize Pt-Co catalysts for methanol electro-oxidation under acidic conditions

Jianhuang Zeng, Jim Yang Lee*

Department of Chemical and Biomolecular Engineering, National University of Singapore, 10 Kent Ridge Crescent, 119260 Singapore

Received 24 June 2004; accepted 19 August 2004
Available online 28 October 2004

Abstract

Carbon-supported Pt-Co and Pt catalysts are prepared by $NaBH_4$ reduction of metal precursors. The particles size of Pt-Co varies with the pH used in the preparation, it is largest (12 nm) in alkaline solution and smallest (3.7 nm) in un-buffered solution. For the latter, X-ray photoelectron spectroscopy shows that Pt exists principally in the metallic state, whereas cobalt is mostly oxidized. The performance of the catalysts for methanol electro-oxidation in acidic media at room temperature is evaluated and compared with that of a Pt/C catalyst. Electrochemical measurements by cyclic voltammetry and chronoamperometry demonstrate consistently high catalytic activities and improved resistance to carbon monoxide for the Pt-Co catalysts, particularly for that prepared in un-buffered solution.

Keywords: Pt-Co; Carbon monoxide resistance; Methanol electro-oxidation; Nanoparticles; Fuel cell; Catalyst

1. Introduction

Among the different types of fuel cell technologies, direct methanol fuel cells (DMFCs) are the most suitable for mobile and portable electronic applications because of their high volumetric energy density, relatively low operating temperature, and the convenience of a liquid fuel that, thereby, enables a greatly simplified system design [1]. One of the major problems of DMFCs is sluggish methanol oxidation kinetics at the anode, which is made worse by the progressive loss of catalytically active sites by CO-like reaction intermediates that are generated during the stepwise dehydrogenation of methanol [2]. It is commonly acknowledged that Pt, as the most common oxidation catalyst for organic molecules including methanol, is highly active for the dehydrogenation reaction, but it is also highly susceptible to CO poisoning [3].

To address the issue of CO poisoning, alloys of Pt with oxophilic metals have been investigated as replacement methanol electro-oxidation catalysts [4]. The increased resistance to CO poisoning is generally explained by a bifunctional mechanism in which the CO-like intermediates on Pt are oxidized by the OH species on the oxophilic metal [5]. Among the binary Pt alloys developed with enhanced catalytic activity and improved CO tolerance in mind, the Pt–Ru [6,7] and Pt–Sn systems [8,9] have been the most extensively investigated. While the effectiveness of the Pt-Sn catalysts is still an ongoing debate [2,10], the Pt-Ru catalysts are generally recognized as the most active methanol electro-oxidation catalyst currently available [6]. The efficiency of DMFCs operating on Pt–Ru is, however, still insufficient for most practical purposes. Furthermore, the supply of Ru [11] and the toxicological effect of Ru remain questionable. Therefore,

* Corresponding author. Tel.: +65 68742899; fax: +65 6779 1936.
E-mail address: cheleejy@nus.edu.sg (J.Y. Lee).

0378-7753/$ – see front matter © 2004 Elsevier B.V. All rights reserved.
doi:10.1016/j.jpowsour.2004.08.022

investigations on alternative Ru-free DMFC anode catalysts continue to be undertaken.

Pt-Co has been used primarily as a magnetic material [12], and an oxygen reduction catalyst [13], and its suitability as a DMFC anode catalyst has not been explored in detail. There has, however, been a report about its performance as a methanol oxidation catalyst under alkaline conditions [14]. Its performance under the more commonly used acidic conditions was only recently assessed using organometallics-derived Pt-Co catalysts [15]. As cobalt is more electropositive than platinum, Pt could withdraw electrons from the neighbouring cobalt atoms and bring about an oxide-cleansing action that places Pt in a more reduced state than in the absence of Co [16]. In this study, carbon-supported Pt-Co catalysts with nanometer particle size and a narrow size distribution are prepared under relatively gentle conditions. The particles size is found to be a function of the pH used in the synthesis. The activity and CO-tolerance of the catalysts in methanol electro-oxidation are evaluated by cyclic voltammetry (CV) and chronoamperometry (CA) in half-cell experiments. The performance is compared with that of a carbon-supported Pt catalyst with the same Pt loading prepared under similar experimental conditions.

2. Experimental

Chloroplatinic acid (H_2PtCl_6) from Aldrich, sodium citrate ($Na_3Cit{\cdot}2H_2O$), sodium boron hydride ($NaBH_4$), cobalt chloride ($CoCl_2$), sulfuric acid (95–97%) and methanol were supplied by Merck. The carbon support was Vulcan XC-72 (BET surface area of 250 $m^2\,g^{-1}$ and average particle size of 40–50 nm) from Cabot. All chemicals were used as received without further purification. De-ionized water was used throughout the study.

2.1. Preparation of electrocatalysts

Thirty milligrams of sodium citrate was added to a mixture of 1 ml of 50 mM of H_2PtCl_6 and 1 ml of 50 mM $CoCl_2$, and then diluted with water to 40 ml. The pH of the as-prepared mix was 5.5. Thirty-six milligrams of Vulcan XC-72 was then introduced followed by 30 min of sonication in an ultrasonic bath. Twenty-two milliliters of solution containing 30 mg $NaBH_4$ was added dropwise to the carbon suspension with stirring at room temperature. Stirring was continued for 6 h before the suspension was filtered to recover the solid product and was washed copiously with water. The recovered solid was then dried in a vacuum oven at 80 °C for 2 h. The catalyst obtained as such is termed as 'Pt-Co/C'. Pt-Co-acidic/C and Pt-Co-basic/C catalysts were prepared following nearly the same procedures except that acids and bases were introduced during the syntheses to adjust the pH to 1.0 and 11.0, respectively. A Pt/C catalyst was also prepared likewise and the Pt loading was kept the same at 20 wt.% for all catalysts.

2.2. Characterization of electrocatalysts

Powder X-ray diffraction (XRD) patterns were recorded on a Rigaku D/Max-3B diffractometer, using CuKα radiation. The X-ray photoelectron spectroscopic (XPS) analysis of samples was conducted on a VG ESCALAB MKII spectrometer using the supplied XPSPEAK software to deconvolute the narrow scan spectra of C, Pt and Co. The elemental compositions of the catalysts were measured by an energy dispersive X-ray (EDX) analyzer attached to a JEOL MP5600LV scanning electron microscope (SEM) that operated at 15 kV. A JOEL JEM2010 transmission electron microscope (TEM) operating at 200 kV was used to examine the particles.

2.3. Electrochemical measurements

The activities of the catalysts were measured by cyclic voltammetry and chronoamperometry by means of an EG&G 273 potentiostat/galvanostat. The working electrode was fabricated by casting Nafion-impregnated catalyst ink on to a 4-mm diameter vitreous glassy carbon disk electrode. A Pt gauze and a saturated calomel electrode (SCE) were used as the counter and the reference electrode, respectively, while the electrolyte was 2 M CH_3OH in 1 M H_2SO_4. All reported potentials were referenced to the SCE. The catalysts were cycled between 0 and 1 V at 50 mV s^{-1} until a stable response was obtained before the cyclic voltammograms and chronoamperograms were recorded.

3. Results and discussion

TEM images of the Pt nanoparticles are shown in Fig. 1, together with those of Pt–Co nanoparticles synthesized under acidic (pH = 1.0), un-buffered (pH = 5.5) and alkaline (pH = 11.0) conditions, respectively. The mean and the standard deviation (σ) of the diameters for the Pt-only nanoparticles are 4.0 and 1.0 nm, respectively. The particle size of the Pt-Co catalysts is strongly dependent on the pH of the solution in which they are formed, with mean diameters of 3.7 (± 0.9), 7.0 (± 3.0) and 12 nm (± 2.3 nm) for Pt-Co/C, Pt-Co-acidic/C and Pt-Co-basic/C, respectively. Hence, Pt–Co nanoparticles synthesized without any pH adjustment have the smallest particle size and a narrow size distribution compared with those of Pt-only nanoparticles.

The size-dependence of the Pt–Co particles on the pH of preparation can be understood as follows. Citric acid is a triprotic acid with $pK_{a1} = 2.8$, $pK_{a2} = 4.2$ and $pK_{a3} = 5.4$, respectively [17]. Citric acid therefore exists as Cit^{3-} in alkaline solutions and as un-dissociated H_3Cit in acidic solutions. At the unadjusted pH of the as-prepared solution (pH = 5.5), H_3Cit, $[H_2Cit]^-$, $[HCit]^{2-}$ and Cit^{3-} coexist, with $[HCit]^{2-}$ and Cit^{3-} as the majority species. The most stable Co^{2+} complex with citrate known to exist in the solution, $[Co(HCit)_2]^{2-}$ [18], cannot therefore be formed under highly acidic or alka-

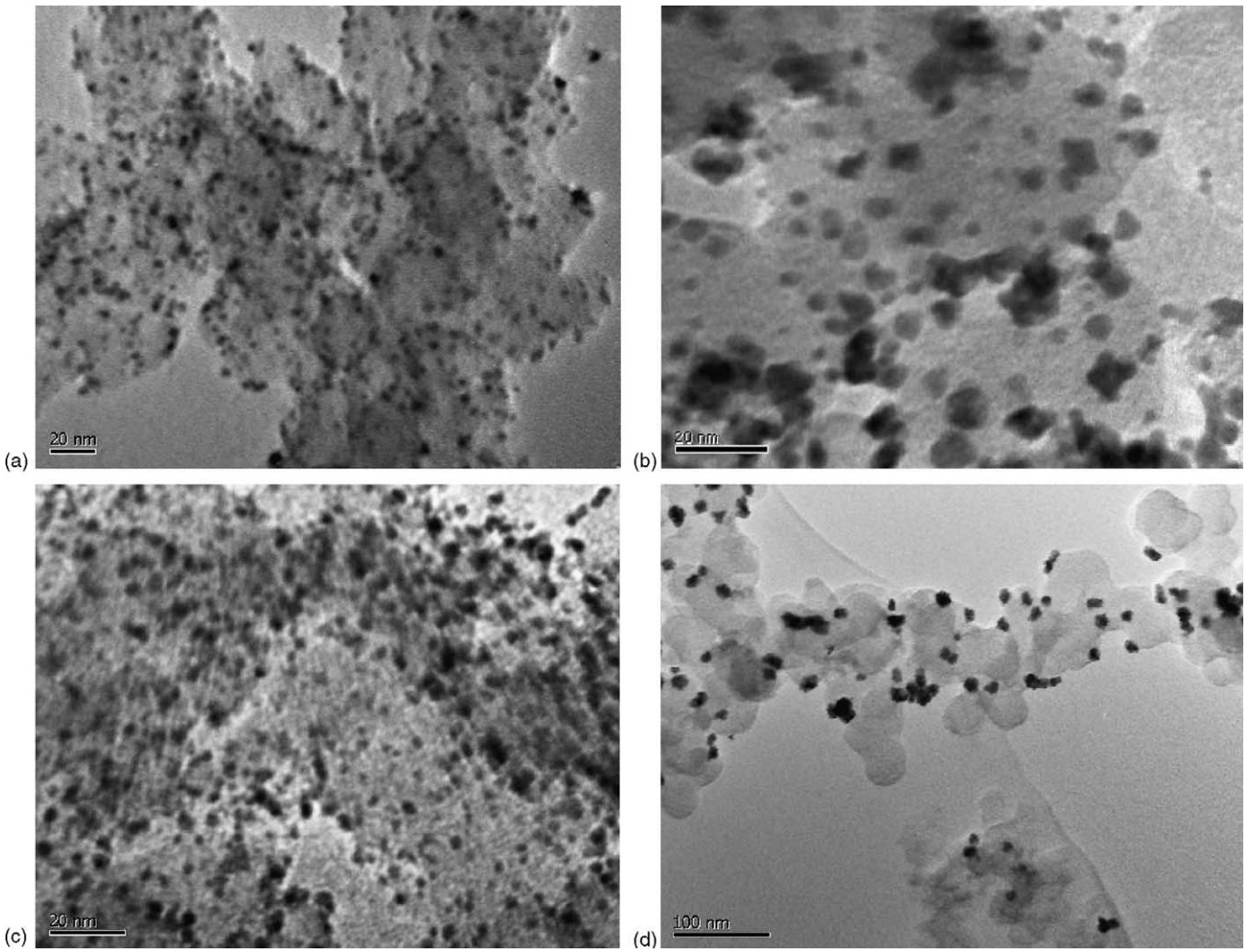

Fig. 1. TEM images of: (a) Pt/C, (b) Pt-Co-acidic/C, (c) Pt-Co/C and (d) Pt-Co-basic/C.

line conditions because of the above-mentioned ionic equilibria of the citric acid. The citrate complexation of Pt^{4+} may likewise be maximized in the un-buffered solution. In addition, the ionic strengths of highly acidic and basic solutions are strongly de-stabilizing for complexes such as $[CoCit]^{-}$ [17].

Since Pt–Co nanoparticles formed in the absence of citrate have large particle sizes and a broad size distribution (data not shown), it may be concluded that the complexation of citrate with metal ions is beneficial to the formation of small particles. In acidic solutions, citrate ions are unable to complex with the metal ions. This results in the release of free Co^{2+} and Pt^{4+} ions that are more facile in $NaBH_4$ reduction, which results in the formation of large metal particles. The reactions in basic solution may proceed through other pathways, but the resulting particles are even larger. Besides serving as a complexing agent, citrate ions also adsorb strongly on the Pt–Co nanoparticles and thereby providing electrostatic stabilization of the latter against particle agglomeration. On the other hand, the amount of citrate used in the Pt-Co synthesis does not appear to influence the particle size or the size-distribution. Cyclic voltammetry also shows that the activities of Pt-Co catalysts with the same Pt loading prepared using different amounts of citrate are largely the same.

EDX analysis of the Pt-Co/C and Pt/C catalysts confirms the Pt loading of 20 wt.% and a nearly 1:1 atomic ratio of Pt to Co. The XRD patterns of the Pt-Co/C and Pt/C catalysts are shown in Fig. 2 for the 2θ range of 30 to 85°. The hexagonal close packed (h.c.p) form of cobalt, if present, would give rise to XRD peaks at $2\theta = 41.7°$ (1 0 0) and 44.8° (1 1 1), whereas the f.c.c form would give rise to a peak at $2\theta = 51.7°$ [19]. Similarly, the presence of f.c.c Pt could be inferred from strong diffractions at $2\theta = 39.7°$ (1 1 1), 46.2° (2 0 0), 67.9° (2 2 0) and 81.0° (2 2 2) [20]. Only four strong peaks at 2θ values of 40.02, 46.30, 68.00 and 81.80° for Pt-Co/C are observed and correspond well with the features of f.c.c Pt, but the cobalt signatures are conspicuously missing. The Pt diffraction peaks are shifted to higher 2θ values and this indicates the formation of a Pt alloy [21]. If Vegard's law is used to interpret the shift in Pt (1 1 1) diffraction from 39.7

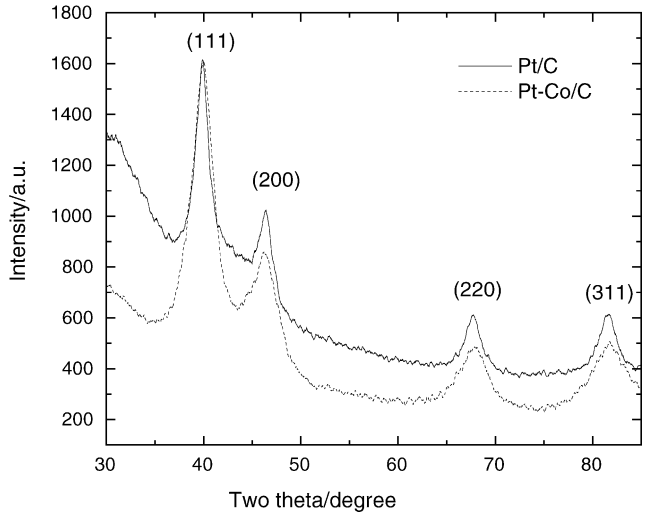

Fig. 2. XRD patterns of Pt-Co/C and Pt/C catalysts.

to 40.02°, then the Pt alloy would contain about 2.4 atom% of cobalt. This would strongly underestimate the 1:1 atomic ratio determined by EDX, but would be similar to the observation of Zhang and coworkers [14]. The discrepancy could be due to the coexistence of unalloyed cobalt or cobalt oxides in the amorphous form. The particle size is calculated by the Debye–Scherrer equation [22]:

$$L = \frac{0.9\lambda_{\mathrm{CuK}\alpha}}{B_{2\theta}\cos\theta_{\max}}$$

where L is the average particle size, $\lambda_{\mathrm{CuK}\alpha}$ the X-ray wavelength, $B_{2\theta}$ the full width at half maximum, and $\theta_{\max}$ the angle at peak maximum. The particle size is 4.1 nm, which agrees fairly well with the TEM measurement (3.7 nm). The lattice parameter was calculated to be 3.922 Å, which is slightly shorter than that of pure Pt (3.924 Å). The shortened lattice parameter (the Pt–Pt distance) is due to the incorporation of Co atoms, and is a well-understood phenomenon for Pt alloys.

The XPS spectra of the Pt-Co/C catalyst in the C 1s, Co $2p_{3/2}$ and Pt 4f regions and the Pt/C catalyst in the Pt 4f region are given in Fig. 3. The binding energies and the relative intensities of the deconvoluted species from the XPS spectra are summarized in Table 1. The C 1s spectrum indicates primarily graphitic carbon (284.24 eV) with about 10% of oxidized carbon as –C=O species (285.44 eV) [23]. Platinum is predominately metallic in both in the Pt-Co/C and Pt/C catalysts with two peaks at 71.36 and 74.66 eV, but the presence

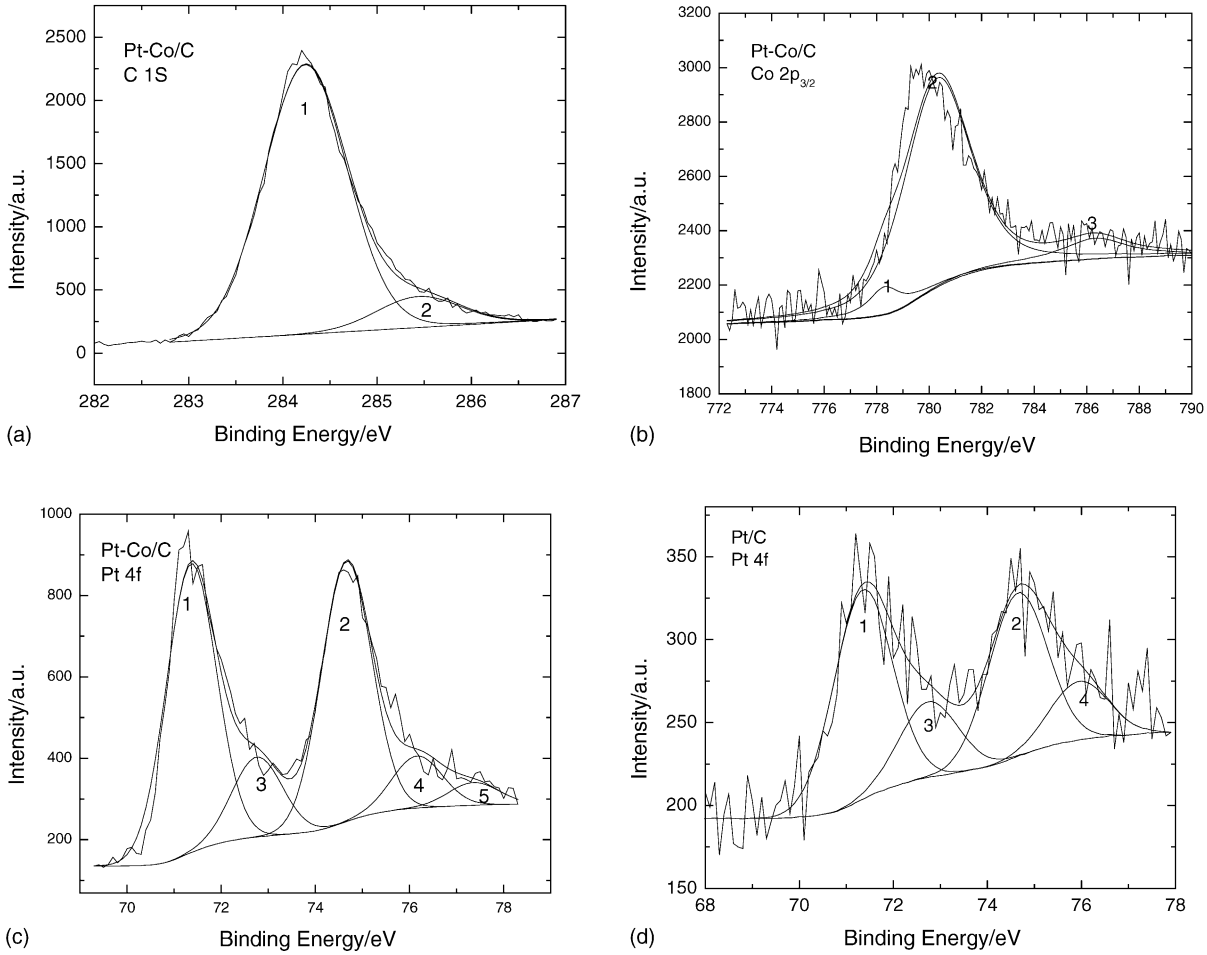

Fig. 3. XPS spectra of Pt-Co/C catalyst in C 1s, Co $2p_{3/2}$ and Pt 4f regions and Pt/C catalyst in Pt 4f region.

Table 1
Surface compositions of Pt-Co/C and Pt/C from deconvolution of the XPS spectra

Catalyst	Species	Binding energy (eV)	Possible chemical state	Relative intensity (%)
Pt-Co/C	C 1s	284.24	Graphite	89.9
		285.44	-C=O like	10.1
	Pt 4f	71.36	Pt^0	41.0
		72.76	PtO	11.4
		74.66	Pt^0	37.0
		76.16	$Pt(OH)_2$	7.4
		77.36	Pt(IV)	3.2
	Co $2p_{3/2}$	778.3	Co^0	6.9
		780.3	$Co(OH)_2$	83.0
		786.3	CoOOH	10.1
Pt/C	Pt 4f	71.36	Pt^0	41.3
		72.76	PtO	14.9
		74.66	Pt^0	32.2
		76.16	$Pt(OH)_2$	11.6

of other peaks indicates some surface oxidation [24]. The percentage of Pt in the zero valent state was 78.0 and 73.5% for the Pt-Co/C and Pt/C catalysts, respectively. The Co $2p_{3/2}$ spectrum in Fig. 3 is more complex, but could be deconvoluted into the three peaks shown in Table 1 with oxidized Co as the predominant species [16]. This contrasts strongly with Pt, where the metallic state predominates. The electronegativity difference between Co and Pt (1.8 and 2.2, respectively) [25] implies an electron-withdrawing effect from Pt to the neighbouring Co atoms, which makes the latter more difficult to reduce. The relatively lower Pt^0 content in the Pt/C catalyst (73.5%) than in the Pt-Co/C catalyst (78.0%) confirms the oxide-cleansing action of Co addition [16]. XPS analysis of a commercial (E-TEK) 40 wt.% Pt-Co/C [16] also shows low metallic Co (6.6%) and high metallic Pt (80.7%) contents. These results are consistent with the XRD data that reveal the limited extent of Co alloying with Pt and the likely existence of amorphous oxides. The Pt to Co ratio from the XPS data worked out to be 1:1.2, which agrees fairly well with the Pt to Co ratio in the initial precursor mixtures (1:1).

The cyclic voltammograms for methanol electro-oxidation on Pt-Co-acidic/C, Pt-Co/C, Pt-Co-basic/C and Pt/C catalysts are presented in Fig. 4. The voltammetric response is fairly typical of electro-oxidation in an acidic medium [26]. The peak at about 0.70 V in the positive-going scan is attributed to the electro-oxidation of methanol. The anodic peak at 0.44 V in the reverse scan can be associated with the reactivation of oxidized Pt [27]. The data in Table 2 show that the Pt-Co catalysts are more active than the Pt-only catalyst, and that the increase in specific activity (normalized with respect to Pt) is more than a surface–area effect. The oxophilic Co may serve as a catalyst promoter. According to the Pourbaix diagrams [28], the corrosion of cobalt is thermodynamically favourable in acidic solutions. The activity enhancement introduced by cobalt addition may be compromised by cobalt leaching after extended operation in the acidic environment of fuel cells if such reaction is not kinetically inhibited.

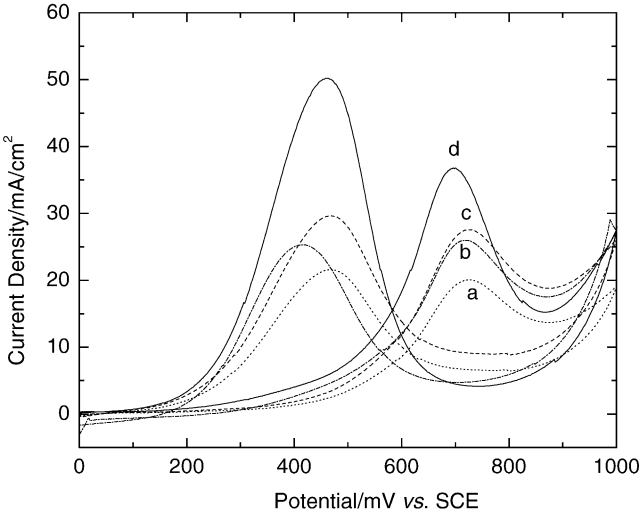

Fig. 4. Cyclic voltammograms of catalysts in 2 M CH_3OH + 1 M H_2SO_4 at room temperature and a scan rate of 50 mV s^{-1}: (a) Pt-Co-basic/C, (b) Pt-Co-acidic/C, (c) Pt/C and (d) Pt-Co/C.

Table 2
Particle attributes and specific activities of Pt/C and various Pt-Co/C catalysts

Catalyst	d_{TEM} (nm)	Specific area (m^2 g^{-1})	Peak current density at 0.7 V (mA cm^{-2})	Specific activity (A m^{-2} Pt)
Pt-Co/C	3.7	76	52	10.0
Pt-Co-acidic/C	7.0	40	25	9.6
Pt-Co-basic/C	12.0	23	22	14.0
Pt/C	4.0	70	31	6.5

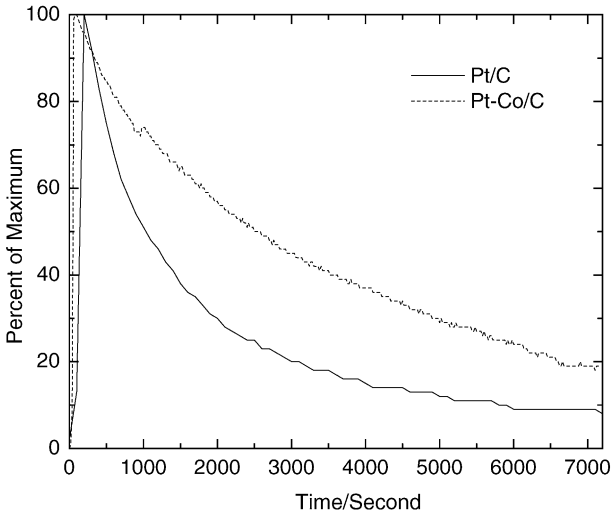

Fig. 5. Chronoamperograms of Pt/C and Pt-Co/C at 0.4 V in 2 M CH_3OH + 1 M H_2SO_4 at room temperature.

The chronoamperograms (CA) of Pt/C and Pt-Co/C catalysts at 0.4 V are compared in Fig. 5. With the potential fixed at 0.4 V, methanol is continuously oxidized on the catalyst surface and tenacious reaction intermediates such as CO_{ads} would begin to accumulate if the kinetics of the removal reaction could not keep pace with that of methanol oxidation. A more gradual decay of current density with time is nevertheless an indication of improved CO resistance. The oxidation current density decreases to 19% of its initial value after 2 h for the Pt-Co/C catalyst as shown in Fig. 5 , whereas the corresponding decay for the Pt/C catalyst is more severe, at 8%. The improved CO-tolerance of the Pt-Co/C catalyst can be categorically explained by a bi-functional mechanism [3,8] in which the reaction between strongly bound Pt_3CO species and OH_{ads} on neighbouring Co sites constitutes the major removal mechanism.

4. Conclusions

Carbon-supported Pt–Co nanoparticles were prepared by the $NaBH_4$ reduction of metal precursors using citric acid as a metal ion complexing agent and a stabilizing agent for the nanoparticles. The metal particle size varies with the pH of the reaction medium; the largest particles are formed in the alkaline solution and the smallest particles (3.7 nm) in the un-buffered solution. The pH sensitivity can be explained by optimum complexation of citrate with metal cations, which influences the kinetics of metal reduction. The addition of cobalt to Pt enhances the specific activity of Pt in methanol oxidation. XPS analyses reveal that Pt mainly exists in the metallic form, while most of the cobalt is oxidized. The activities of the Pt-Co catalysts in methanol electro-oxidation under acidic conditions, as measured by cyclic voltammetry and chronoamperometry, confirm the beneficial effect of Co addition to Pt where improvements in both activity and CO-tolerance are realizable.

References

[1] P. Costamagna, S. Srinivasan, J. Power Sources 102 (2001) 242–252.
[2] S. Wasmus, A. Kuver, J. Electroanal. Chem. 461 (1999) 14–31.
[3] N.M. Markovic, H.A. Gasteiger, P.N. Ross, X. Jiang, I. Villegas, M.J. Weaver, Electrochim. Acta 141 (1995) 91–98.
[4] A. Lima, C. Coutanceau, J.-M. Leger, C. Lamy, J. Appl. Electrochem. 31 (2001) 379–386.
[5] H.A. Gasteiger, N.M. Markovic, P.N. Ross Jr., E.J. Cairns, Electrochim. Acta 39 (1994) 1825–1832.
[6] Y.C. Liu, X.P. Qiu, Z.G. Chen, W.T. Zhu, Electrochem. Commun. 4 (2002) 550–553.
[7] Z.L. Liu, J.Y. Lee, M. Han, W.X. Chen, L.M. Gan, J. Mater. Chem. 12 (2002) 2453–2458.
[8] K. Wang, H.A. Gasteiger, N.M. Markovic, P.N. Ross Jr., Electrochim. Acta 41 (1996) 2587–2593.
[9] M. Gotz, H. Wendt, Electrochim. Acta 43 (1998) 3637–3644.
[10] W.J. Zhou, B. Zhou, W.Z. Li, Z.H. Zhou, S.Q. Song, G.Q. Sun, Q. Xin, S. Douvartides, M. Goula, P. Tsiakaras, J. Power Sources 126 (2004) 16–22.
[11] T. Ioroi, K. Yasuda, Z. Siroma, N. Fujiwara, J. Electrochem. Soc. 150 (2003) A1225–A1230.
[12] A. Kumbhar, L. Spinu, F. Agnoli, K.Y. Wang, W.L. Zhou, C.J. O'Connor, IEEE Trans. Magn. 37 (2001) 2216–2218.
[13] M.K. Min, J. Cho, K. Cho, H. Kim, Electrochim. Acta 45 (2000) 4211–4217.
[14] X. Zhang, K.-Y. Chan, J. Mater. Chem. 12 (2002) 1203–1206.
[15] T. Okada, Y. Suzuki, T. Hirose, T. Ozawa, Electrochim. Acta 49 (2004) 385–395.
[16] A.S. Arico, A.K. Shukla, H. Kim, S. Park, M. Min, V. Antonucci, Appl. Surf. Sci. 172 (2001) 33–40.
[17] M. Borkowski, G.R. Choppin, R.C. Moore, S.J. Free, Inorg. Chim. Acta 298 (2000) 141–145.
[18] IUPAC, Stability constants of metal-ion complexes: part B, Organic Ligands, Pergamon Press, 1979, p. 361.
[19] F. Guo, H.G. Zheng, Z.P. Yang, Y.T. Qian, Mater. Lett. 56 (2002) 906–909.
[20] X.W. Teng, H. Yang, J. Am. Chem. Soc. 125 (2003) 14559–14563.
[21] S.-A. Lee, K.-W. Park, J.-H. Choi, B.-K. Kwon, J. Electrochem. Soc. 149 (2002) A1299–A1304.
[22] B.D. Cullity, Elements of X-Ray Diffraction, Addison-Wesley, London, 1978, p. 81.
[23] A.S. Arico, Z. Poltarzewski, H. Kim, A. Morana, N. Giordano, V. Antonucci, J. Power Sources 55 (1995) 159–166.
[24] A.K. Shukla, M. Neergat, P. Bera, V. Jayaram, M.S. Hegde, J. Electroanal. Chem. 504 (2001) 111–119.
[25] K.M. Ralls, T.H. Courtney, J. Wulff, Introduction to Materials Science and Engineering, John Wiley & Sons, New York, 1938, p. 53.
[26] W.X. Chen, J.Y. Lee, Z.L. Liu, Chem. Commun. (2002) 2588–2589.
[27] X. Zhang, K.Y. Chan, Chem. Mater. 15 (2003) 451–459.
[28] M. Pourbaix, Atlas of Electrochemical Equilibria in Aqueous Solutions, Pergamon Press, Brussels, 1963, p. 322.